Dzyaloshinsky-Moriya interaction and long lifetime of the spin state in the Cu_{3} triangular spin cluster by inelastic neutron scattering measurements

K. Iida, Y. Qiu, and T. J. Sato

Phys. Rev. B **84**, 094449 — Published 28 September 2011

DOI: 10.1103/PhysRevB.84.094449

Dzyaloshinsky-Moriya interaction and long lifetime of the spin state in the Cu_3 triangular spin cluster by inelastic neutron scattering measurements

K. Iida[1],* Y. Qiu[2,3], and T. J. Sato[1]
[1]*Neutron Science Laboratory, Institute for Solid State Physics, University of Tokyo, Kashiwa, Chiba 277-8581, Japan*
[2]*NIST Center for Neutron Research, National Institute of Standards and Technology, Gaithersburg, Maryland 20899, USA and*
[3]*Department of Materials Science and Engineering, University of Maryland, College Park, Maryland 20742, USA*
(Dated: September 7, 2011)

Inelastic neutron scattering (INS) experiments have been performed on the Cu_3 triangular molecular nanomagnet using powder samples. In the medium resolution INS experiment, two peaks were observed at $\hbar\omega = 0.5$ and 0.6 meV, whereas an additional excitation peak was detected at very low energy $\hbar\omega = 0.1$ meV in the higher resolution experiment. A model Hamiltonian and its optimum interaction parameters were determined from the observed peak position, width, and intensity. A key ingredient of the model Hamiltonian is Dzyaloshinsky-Moriya interactions as suggested in the earlier reports, which is now directly evidenced by the observation of the 0.1 meV peak, corresponding indeed to a splitting of ground state quartet into two doublets. Temperature dependences of integrated intensity of the 0.5 and 0.6 meV peaks are well reproduced by the Boltzmann distribution function up to 10 K, above which a small deviation was detected. Nevertheless, the inelastic peaks were visible even at very high temperatures as 50 K, indicating extraordinary weak coupling between spins and lattice vibrations (or any other perturbations) compared to the other known molecular nanomagnets.

PACS numbers: Valid PACS appear here
Keywords:

I. INTRODUCTION

Quantum fluctuation in magnetic systems is strongly enhanced by reducing system size, and intriguing nanoscale quantum effect may emerge in finite size quantum spin systems. A molecular nanomagnets[1] is a system of isolated spin clusters, where each spin cluster comprises a finite number of interacting spins. The quantum effect may be amplified due to the small system size, and therefore, in a hope that they provide a rich playground to investigate intriguing nanoscale quantum phenomena, molecular nanomagnets have been intensively studied to date.

Classical examples of molecular nanomagnets may be Mn_{12}[2,3] and Fe_8,[4] where quantum-mechanical tunneling of bulk magnetization was observed at low temperatures. This macroscopic quantum tunneling is now understood as due to a quantum tunneling between the z-component of the ground-state total spin across the Ising anisotropy barrier. Another interesting examples may be the molecular grid nanomagnet Mn-$[3\times3]$[5,6] and the antiferromagnetic heterometallic ring Cr_7Ni,[7] showing a quantum coherence between the total spin states. In these systems, coherent oscillation of the total states $S_{\rm total}$ and $S_{\rm total}+1$ was observed at level (anti-) crossing field; such a fluctuation between different $S_{\rm total}$ can be usually neglected in macroscopic antiferromagnets, although $S_{\rm total}$ is not strictly conservable for Heisenberg Hamiltonian.

Quantum effect may be seen in non-equilibrium states. Recently, it has been found that $S = 1/2$ spin trimer clusters, such as V_3,[8] Cu_3As,[9] and Cu_3Sb,[10,11] show a half-step magnetization change, that is, the magnetization m changes stepwise with the height $\Delta m = 1\ \mu_{\rm B}$. It should be noted that a reversal of even a single $S = 1/2$ spin changes the magnetization by $\Delta m = 2\ \mu_{\rm B}$ [assuming $g = 2$], and therefore, such fractionalized magnetization change should certainly be due to intriguing quantum effect. Moreover, the half-step magnetization process can only be observed in pulsed magnetic field, and is accompanied by a milli-second-order hysteresis, indicating its non-equilibrium nature.

Exemplified by the Cu_3Sb cluster (hereafter, Cu_3 in short),[14] earlier studies are summarized as follows. The chemical formula is $Na_{12}[Cu_3(SbW_9O_{33})_2\ (H_2O)_3]\cdot46H_2O$. Three Cu^{2+} ions are placed at the distances of $d_{1,2} = d_{2,3} = 4.871$ and $d_{3,1} = 4.772$ Å as shown in Fig. 1(a). To date, several measurements have been performed, such as magnetic susceptibility, magnetization in pulsed field, electron spin resonance (ESR), and nuclear magnetic resonance.[10,11] The magnetic susceptibility measurement suggests dominant antiferromagnetic coupling between the Cu^{2+} ions with $S = 1/2$, whereas the half-step magnetization change was observed in pulse field as noted above. The exchange path is thought to be Cu-O-W-O-W-O-Cu.[10] There is no inversion symmetry at the center of any two Cu^{2+} ions, suggesting the existence of the Dzyaloshinsky-Moriya (DM) interaction in addition to the super exchange interactions; the DM interaction was indeed inferred in the field-direction dependence of the ESR parameters. The spin-lattice relaxation rate $1/T_1$ shows weak enhancement at 2 and 4.5 T, from which strong spin-lattice coupling is inferred.

To explain the above bulk measurements, as well as the half-step magnetization change, the following spin Hamiltonian has been proposed:[11]

$$\mathcal{H} = \sum_{i=1}^{3}\left[-\sum_{\alpha}^{x,y,z}\left(J_{i,i+1}^{\alpha}S_i^{\alpha}S_{i+1}^{\alpha}\right)+\mathbf{D}_{i,i+1}\cdot(\mathbf{S}_i\times\mathbf{S}_{i+1})\right] + \mu_{\mathrm{B}}\sum_{i=1}^{3}\mathbf{S_i}\cdot\tilde{g}\cdot\mathbf{B}, \quad (1)$$

where $J_{i,i+1}^{\alpha}$ and $D_{i,i+1}^{\alpha}$ are the α-component of the exchange and DM interactions between the i-th and $(i+1)$-th Cu^{2+} ions, and μ_{B} is the Bohr magneton. With the proposed interaction parameters, energy level scheme consists of a ground state with $S_{\mathrm{total}} = 1/2$, a first excited state with $S_{\mathrm{total}} = 1/2$ at 100 μeV higher than the ground state, and a $S_{\mathrm{total}} = 3/2$ quartet at 580 μeV weakly split into two doublets.[11] The splitting of the two $S_{\mathrm{total}} = 1/2$ doublets is due to the DM interaction, and is suggested to be a key to understand the half-step magnetization.[12,13] The two degenerated ground-state wave functions have different chirality; one has an antilevel crossing with $S_{\mathrm{total}} = 3/2$ states, but the other has only small admixture. Consequently, above the level crossing field [$B > 4.5$ T], both the $S_{\mathrm{total}} = 1/2$ and 3/2 states may equally populated, resulting in the average magnetization of 2 μ_{B}. The $S_{\mathrm{total}} = 1/2$ state is metastable above the level crossing field, and thus the observed half-step magnetization change in milli-second field sweep suggests that the relaxation of $S_{\mathrm{total}} = 1/2$ to 3/2 state is extraordinary slow.

This way, the observed bulk properties of the Cu_3 cluster are reasonably explained by the above model Hamiltonian. Nonetheless, the obtained Hamiltonian parameters should be confirmed in much microscopic manner, since the bulk measurements only uses the excitation energies so that misassignment of energy levels may happen. We, therefore, employ neutron inelastic scattering to conclusively determine the model Hamiltonian and its optimum parameters. Origin of the long lifetime of the spin state is another issue, which has to be elucidated by directly observing the lifetime of the excitation levels, *i.e.*, the broadening of the excitation peaks in INS spectra. In this paper, we report our detailed neutron scattering investigation on the Cu_3 spin cluster; we provide conclusive parameters of the model Hamiltonian, and also give an insight into the origin of the long lifetime of the spin state.

II. EXPERIMENTAL DETAILS

The powder sample was prepared using the procedure reported in the Refs. 14 and 15, and the deuterated powder sample was also prepared for the high-energy-resolution INS measurement. Magnetic susceptibility measurement on 45.3 mg non-deuterated powder sample was performed using a SQUID magnetometer in the temperature range of $1.8 \leq T \leq 300$ K.

A part of INS experiments was performed using the triple-axis spectrometer ISSP-HER, installed at the JRR-3 research reactor (Tokai, Japan). About 18.2 g non-deuterated powder sample was used in those experiments. We have employed vertically focusing monochromator to select incident neutron wavelength, whereas double focusing (*i.e.* both horizontal and vertical focusing) technique was used for the analyzer. Pyrolytic graphite (PG) 002 reflections were used both for the monochromator and analyzer. The spectrometer was operated in the fixed-final-energy mode with $E_{\mathrm{f}} = 2.4$ meV, resulting in the instrumental resolution of 61 μeV (FWHM, or full width at half maximum) at the

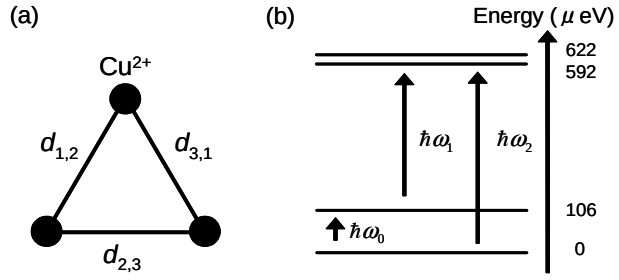

FIG. 1: (a) A structure of the Cu_3 spin cluster, where each circle represents the Cu^{2+} ion. The distances between Cu^{2+} ions $d_{1,2}$, $d_{2,3}$, and $d_{3,1}$ are written in the text. (b) Schematic view of the energy levels of the model Hamiltonian obtained by the optimum parameters given in Eq. (2). $\hbar\omega_0$ represents the splitting between the two low-lying $S_{\mathrm{total}} = 1/2$ spin doublets by the DM interaction, whereas $\hbar\omega_1$ and $\hbar\omega_2$ correspond to the INS peaks at 0.5 and 0.6 meV in the INS spectra measured at HER as shown in Fig. 2.

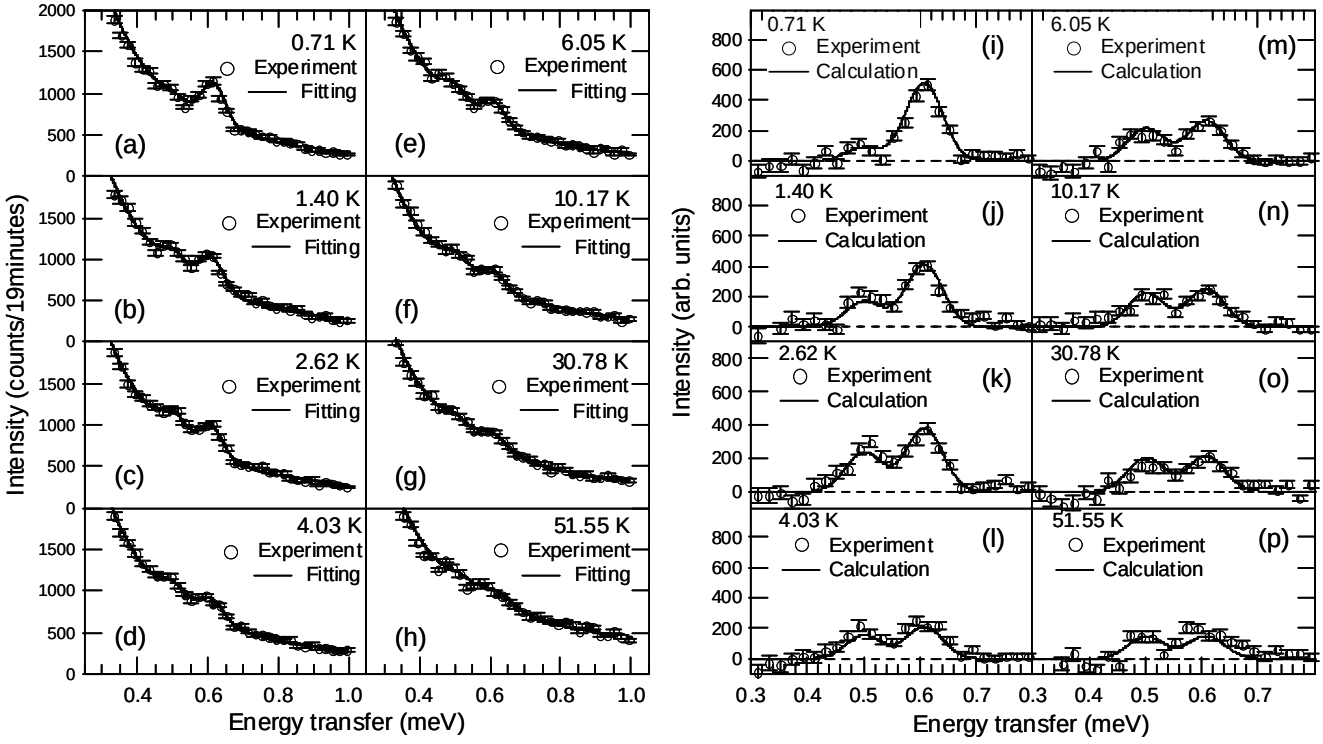

FIG. 2: The INS spectra of $Q = 0.95$ Å^{-1} at (a) $T = 0.71$, (b) 1.40, (c) 2.62, (d) 4.03, (e) 6.05, (f) 10.17, (g) 30.78, and (h) 51.55 K measured at HER and the fitting results (details are written in text). The error bars in here and all subsequent figures represent one standard deviation. The background subtracted INS spectra measured at HER and the calculated intensities using Eq. (2) in Ref. 18 of $Q = 0.95$ Å^{-1} at (i) $T = 0.71$, (j) 1.40, (k) 2.62, (l) 4.03, (m) 6.05, (n) 10.17, (o) 30.78, and (p) 51.55 K are illustrated.

elastic position. The resolutions at $\hbar\omega = 0.49$ and 0.60 meV were estimated as 68 and 71 μeV (FWHM), assuming the Cooper-Nathans type resolution function.[16] The higher harmonic neutrons were eliminated using the cooled Be filter. The non-deuterated powder sample was sealed in the aluminum sample can filled with the ^{4}He exchange gas, and then was set to a closed-cycle ^{3}He refrigerator with the lowest working temperature of about 0.7 K.

A supplemental INS experiment was also performed using the disk chopper time-of-flight spectrometer DCS installed at NIST Center for Neutron Research (Gaithersburg, USA) with $E_{\rm i} = 1.0$ meV. The resolution at elastic position was 18.7 μeV (FWHM), and the resolutions at $\hbar\omega = -0.1$ and 0.1 meV were estimated as 22.6 and 15.1 μeV (FWHM), respectively.[17] The deuterated powder sample of about 4.7 g was put in the aluminum sample can, and set to the ILL Orange cryostat, with which the lowest working temperature was 1.5 K.

III. EXPERIMENTAL RESULTS

First, INS spectrum at $Q = 0.95$ Å^{-1} and $T = 0.71$ K was measured at HER. The result is shown in Fig. 2(a). Strong incoherent scattering from hydrogen is found at the elastic position, which gives rise to considerable background at low energies. Nevertheless, a clear peak was observed at 0.6 meV, in addition to a weak hump around 0.5 meV. The INS spectra at elevated temperatures are also shown in Figs. 2(b)-2(h). As seen in the figures, the lower energy hump at 0.5 meV once becomes a much clearer peak as temperature is increased, and then broadened above 10 K. On the other hand, the higher energy peak at 0.6 meV loses its intensity monotonically. To quantitatively discuss the excitation energy and intensity, and also to obtain a profile function of the non-magnetic background, we performed least-square fitting to a model scattering function; two Gaussian functions with peak energies $\hbar\omega_1$ and $\hbar\omega_2$ were assumed for the two inelastic peaks, while the incoherent background was modeled as the sum of Gaussian and Lorentzian functions centered at zero-energy transfer. We fit all the spectra at different temperatures, $T = 0.71$, 1.40, 2.62, 4.03, 6.05, 10.17, 30.78, and 51.55 K simultaneously, where $\hbar\omega_1$ and $\hbar\omega_2$ are assumed to be global parameters. The fitting results are shown by the solid lines in the Figs. 2(a)-2(h). A good coincidence to the observed spectra is apparent at all the temperatures up to 51.55 K. We obtained peak positions as $\hbar\omega_1 = 0.498(2)$ and $\hbar\omega_2 = 0.607(1)$ meV. We note that

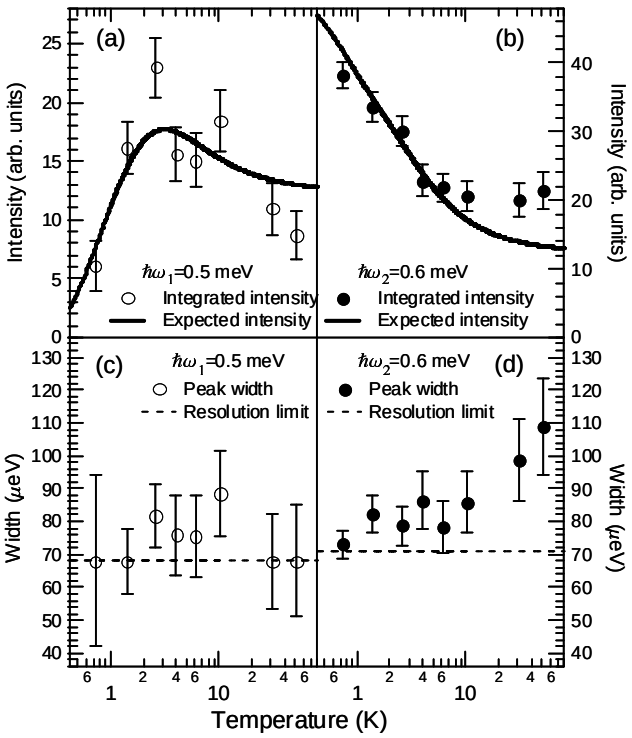

FIG. 3: The integrated and expected intensities of the peaks at (a) $\hbar\omega = 0.5$ and (b) 0.6 meV. The widths of the INS peaks and the resolution-limited widths at (c) $\hbar\omega = 0.5$ and (d) 0.6 meV.

the reported result[11] expects the excitation energies as $\hbar\omega = 0.484$ and 0.584 meV, which almost correspond to the present INS result. This fact confirms that these excitations originate from the Cu_3 spin cluster.

Temperature dependences of the integrated intensity and peak width were also obtained in the above fitting. The integrated intensity for the 0.5 and 0.6 meV peaks is shown in Figs. 3(a) and 3(b), respectively. Different temperature dependences are readily seen in the figures. As already noted from the raw spectra, the 0.6 meV peak monotonously weakens, whereas the intensity of the 0.5 meV peak shows a maximum around 3 K. The peak widths for the two excitations are also shown in Figs. 3(c) and 3(d). At the lowest temperature, the widths for both the peaks are identical to the instrumental resolution shown by the dotted lines, indicating infinitely long lifetime for both the ground and excited states. As temperature is elevated, a clear increasing behavior can be seen for the 0.6 meV peak. On the other hand, the width seems to be mostly temperature independent for the 0.5 meV peak, although the large uncertainty, resulting from relatively insufficient statistics, makes any quantitative discussion difficult. It may be noteworthy that the width of the 0.6 meV peak shows steeper increase above 10 K, indicating that the lifetime of ground and/or excited states becomes suddenly shorter. The temperature dependences of the intensity and width will be further discussed in the next section.

Inelastic spectrum at lower energy regions was then investigated using DCS with higher energy resolution. Figure 4 shows the INS spectra of deuterated powder Cu_3; $S(Q, \hbar\omega)$ at $T = 1.5$ and 30 K is integrated in the range of $0.1 \leq Q \leq 1.3$ Å^{-1}. Another INS peak was observed in this low energy range at $\hbar\omega = 0.1$ meV in the $T = 1.5$ K spectrum. This peak almost disappears in the higher temperature spectrum, indicating its magnetic origin. We then fitted the INS spectra with a model function consisting of incoherent background centered at the elastic position, as well as an inelastic Gaussian function. The fitting results for both the temperatures are shown by the solid lines in Fig. 4; a satisfactory coincidence can be seen in the figures. The peak position was determined as $\hbar\omega = 0.103(2)$ meV in the fitting. From the above experimental results, we conclude that there are three inelastic peaks in the Cu_3 system at the lowest temperature, appearing at $\hbar\omega = 0.103(2), 0.498(2)$ and 0.607(1) meV.

IV. DISCUSSION

In this section, we first determine the parameters in Eq. (1) using the medium-resolution data including the two excitation peaks at $\hbar\omega = 0.5$ and 0.6 meV. Then, we show that the low-energy excitation at $\hbar\omega_0 \simeq 0.1$ meV, observed

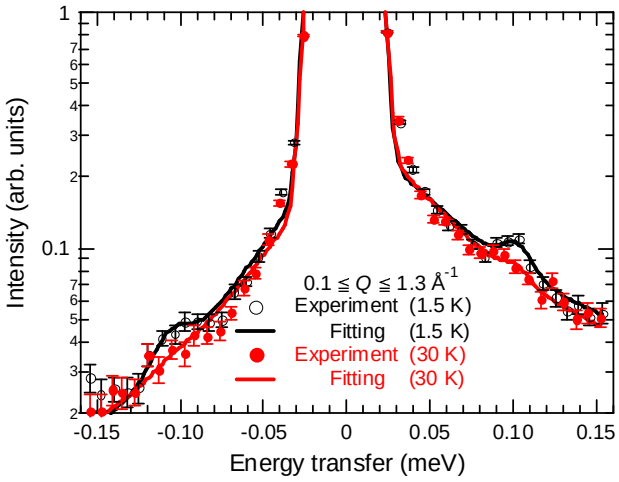

FIG. 4: (Color online) The INS spectra of $0.1 \leq Q \leq 1.3$ Å^{-1} at $T = 1.5$ and 30 K measured at DCS using deuterated powder Cu_3. We use a log scale for the vertical axis. Both spectra are fitted by the similar procedure in Figs. 2(a)−2(h).

in the high-energy-resolution neutron experiment, can be perfectly reproduced by the determined model Hamiltonian. Finally, we discuss the temperature dependences of the INS peaks at $\hbar\omega = 0.5$ and 0.6 meV to elucidate the origin of the long lifetime of the spin state in the Cu_3 cluster.

A. Hamiltonian parameter determination

For the Hamiltonian parameter determination, here we perform a whole profile fitting to the observed inelastic scattering spectra in a wide temperature range, instead of using the Gaussian-fit results described in the former section. In the whole profile fitting, not only the excitation energies, but also the relative intensity and their temperature dependence will be included in the fitting procedure. Therefore, this method will reduce the chance of misassigning the excitation levels, compared to just using excitation peak energies as usually done in earlier studies. The procedure to calculate the neutron scattering function from the given model Hamiltonian Eq. (1) was reported in Ref. 18, where Eq. (2) defines the calculated intensity $I^{\rm cal}(Q, \hbar\omega)$. We also used the magnetic form factor of Cu^{2+} ions given in Ref. 19. To obtain optimum Hamiltonian parameters, we only used the experimental data below 10 K, where the intrinsic peak widths are very small compared to the instrumental resolution, as discussed before. Hence, we assume that the INS peaks have the instrumental-resolution widths in the present calculations for $I^{\rm cal}(Q, \hbar\omega)$.

For the actual fitting, we first subtract the background from the raw spectra, using the estimated background profile function in the previous section. The background subtracted spectra are shown in Figs. 2(i)−2(p). The least-squares fitting was then performed to the background subtracted spectra at $T = 0.71$, 1.40, 2.62, 4.03, 6.05, and 10.17 K. The resulting calculated scattering intensity $I^{\rm cal}(Q, \hbar\omega)$ is shown by the solid lines in the figures. The satisfactory correspondence found in the figures ensures the reliability of the estimated parameters. The obtained optimum parameters are as follows:

$$\begin{aligned} J^x_{1,2} = J^y_{1,2} = J^x_{2,3} = J^y_{2,3} &= -4.19 \pm 0.03 \text{ K}, \\ J^z_{1,2} = J^z_{2,3} &= -4.67 \pm 0.05 \text{ K}, \\ J^x_{3,1} = J^y_{3,1} &= -4.14 \pm 0.01 \text{ K}, \\ J^z_{3,1} &= -4.42 \pm 0.02 \text{ K}, \\ D^z_{1,2} = D^z_{2,3} = D^z_{3,1} &= 0.66 \pm 0.01 \text{ K}, \\ D^x_{1,2} = D^y_{1,2} &= 0.55 \pm 0.05 \text{ K}. \end{aligned} \tag{2}$$

The uncertainty ranges of the obtained parameters were estimated as the standard deviation of the Gaussian distribution using the linear approximation. The energy levels calculated using the optimum parameters are shown in Fig. 1(b). The $S_{\rm total} = 3/2$ states are almost degenerated whereas the $S_{\rm total} = 1/2$ quartet is split into two doublets. The excitations, $\hbar\omega_0$, $\hbar\omega_1$, and $\hbar\omega_2$ are estimated as 0.106, 0.501, and 0.607 meV, respectively. It should be noted that the optimum parameters are within 10% difference from the reported parameters[11], and hence the estimated

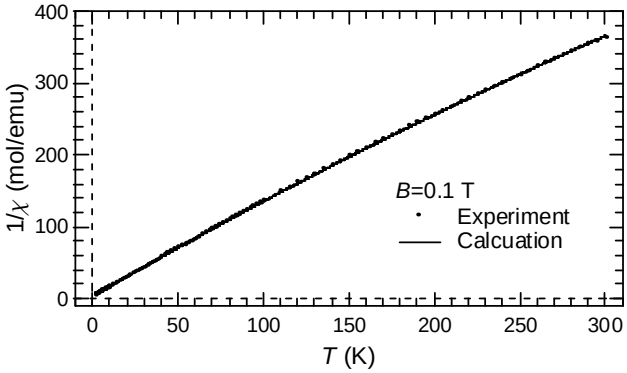

FIG. 5: The experimental and calculated $1/\chi$ in $B = 0.1$ T.

excitation energies are almost the same. We should note that the spin Hamiltonian containing only exchange interaction can give the same quality fit with the following parameters: $J^x_{1,2}/\mathrm{K} = -4.69 \pm 0.01$, $J^z_{1,2}/\mathrm{K} = -4.68 \pm 0.01$, $J^x_{3,1}/\mathrm{K} = -3.10 \pm 0.01$, and $J^z_{3,1}/\mathrm{K} = -4.21 \pm 0.04$. However, this Hamiltonian cannot reproduce the avoided level crossing when the ground state changes to the $S_{\mathrm{total}} = 3/2$ state. Therefore, we choose the parameters given in Eq. (2).

As seen in the energy level scheme given in Fig. 1(b), the low energy excitation at $\hbar\omega = 0.106$ meV is now expected. It should be emphasized that this excitation is between the two $S_{\mathrm{total}} = 1/2$ doublets, which can only split due to the DM interaction; anisotropy of the exchange interaction $[J^x_{i,i+1} \neq J^z_{i,i+1}]$ may split the $S_{\mathrm{total}} = 3/2$ quartet, resulting in the 0.5 and 0.6 meV peak in the INS spectrum, however this cannot give rise to the 0.1 meV peak at the lowest temperature. Since we clearly see the inelastic peak at $\hbar\omega = 0.103(2)$ meV,[20] *i.e.* the ground state splitting, as shown in Fig. 4, we conclude that the DM interaction surely exists in the Cu_3 spin cluster. The splitting of the ground state quartet is of the similar magnitude as that in V_3.[18]

It should be mentioned that there is another energy transfer at $\hbar\omega = 0.03$ meV between the slightly split $S_{\mathrm{total}} = 3/2$ quartet, and this may be observed at high temperatures. However, the intensity of the 0.03 meV peak at $T = 30$ K is expected as half of that of the 0.1 meV peak at $T = 1.5$ K. In addition, the expected excitation energy 0.03 meV is too low where the background becomes serious in the present spectrometer configuration. Therefore, it is quite reasonable that we did not see the excitation between the weakly split $S_{\mathrm{total}} = 3/2$ quartet in the spectrum at $T = 30$ K.

To further check the reliability of the model Hamiltonian, temperature dependence of the susceptibility $(1/\chi)$ is calculated using the optimum parameters. In the calculation of the susceptibility, we use the reported value of the g tensor[11] in Eq. (1). Figure 5 illustrates the comparison between observed susceptibility of the powder sample and the calculated susceptibility. The observed susceptibility is well reproduced by the calculation in the wide temperature range, again confirming the validity of the present parameter estimation.

B. Spin-lattice coupling

Next, we discuss the temperature dependences of the INS peaks measured at HER in detail. As already shown in Figs. 3(a) and 3(b), different temperature dependence is readily seen for the 0.5 and 0.6 meV peaks. The 0.5 meV peak originates from the transition between the upper $S_{\mathrm{total}} = 1/2$ state and the $S_{\mathrm{total}} = 3/2$ states, whereas the 0.6 meV peak from that between the lower $S_{\mathrm{total}} = 1/2$ and $S_{\mathrm{total}} = 3/2$. The temperature dependence of the intensity of each peak should obey the Boltzmann factor of the initial state as far as other perturbations are negligible. Hence, we calculate the expected intensity solely from the Boltzmann population factor, and compare it to the experimental observation.

In Figs. 3(a) and 3(b), the calculated intensity is over plotted to the observed integrated intensity. The observation and calculation for both the INS peaks are in agreement below 10 K, whereas they are not above 10 K. This feature coincides with the pronounced increase of the peak widths for the 0.6 meV peak above 10 K, as already seen in Fig. 3(d). As already pointed out earlier, such a broader width suggests that the relaxation time of the spin state becomes considerably shorter above 10 K. Thus, the spin-lattice coupling (or any other perturbation to the spin system) may become relatively relevant above 10 K. Nonetheless, it should be noted that the 0.5 and 0.6 meV inelastic peaks were definitely visible at high temperatures as 50 K with only broadening. Moreover, the spin Hamiltonian Eq. (1) can reproduce the magnetic susceptibility up to very high temperature as 300 K. These results suggest that the perturbative term is not dominant even above 10 K. Therefore, the spin state is only weakly influenced by the lattice

vibration (or other perturbations), and in particular below 10 K the perturbation is negligible, at least in the present neutron time scale. It is very intriguing to study the origin of this decoupling between the phonon and spin states, and is left for future study.

V. CONCLUSIONS

INS experiments have been performed on the Cu_3 triangular spin cluster using powder samples. First, from the INS spectra measured at HER, we obtained the optimum parameters of the spin Hamiltonian listed in Eq. (2). Secondly, we have directly observed the splitting of the ground state quartet due to the DM interaction at 0.1 meV, the energy exactly expected from the optimum parameters. Thirdly, the temperature dependences of the INS peaks at 0.5 and 0.6 meV suggest that the spin-lattice coupling in Cu_3 is weak, resulting in the rigid spin state, or the long lifetime of the spin state at low temperatures. We, thus, conclude that they are the key features to explain the half-step magnetization change with the milli-second order hysteresis.

Acknowledgements

One (K.I.) of us acknowledges for Global COE Program "the Physical Sciences Frontier", MEXT, Japan. We also acknowledge for the financial support from the US-Japan Cooperative Program on Neutron Scattering. Work at NCNR is in part supported by the National Science Foundation under Agreement No. DMR-0454672. We would like to thank N. Aso, M. Yokoyama, T. Asami, Y. Kawamura, and J. R. D. Copley for their help in our INS experiments.

---

* Electronic address: ki7e@virginia.edu; Present address: Department of Physics, University of Virginia, Charlottesville, Virginia 22904, USA.

[1] D. Gatteschi, R. Sessoli, and J. Villain, *Molecular Nanomagnet* (OXFORD university press, 2006).
[2] L. Thomas, F. Lionti, R. Ballou, D. Gatteschi, R. Sessoli, and B. Barbara, Nature (London) **383**, 145 (1996).
[3] J. R. Friedman, M. P. Sarachik, J. Tejada, and R. Ziolo, Phys. Rev. Lett. **76**, 3830 (1996).
[4] S. Takahashi, J. van Tol, C. C. Beedle, D. N. Hendrickson, L.-C. Brunel, and M. S. Sherwin, Phys. Rev. Lett. **102**, 087603 (2009).
[5] O. Waldmann, S. Carretta, P. Santini, R. Koch, A. G. M. Jansen, G. Amoretti, R. Caciuffo, L. Zhao, and L. K. Thompsson, Phys. Rev. Lett. **92**, 096403 (2004).
[6] T. Guidi, S. Carretta, P. Santini, E. Liviotti, N. Magnani, C. Mondelli, O. Waldmann, L. K. Thompson, L. Zhao, C. D. Frost, G. Amoretti, and R. Caciuffo, Phys. Rev. B **69**, 104432 (2004).
[7] S. Carretta, P. Santini, G. Amoretti, T. Guidi, J. R. D. Copley, Y. Qiu, R. Caciuffo, G. Timco, and R. E. P. Winpenny, Phys. Rev. Lett. **98**, 167401 (2007).
[8] T. Yamase, E. Ishikawa, K. Fukaya, H. Nojiri, T. Taniguchi, and T. Atake, Inorg. Chem. **43**, 8150 (2004).
[9] K. Y. Choi, Y. H. Matsuda, H. Nojiri, U. Kortz, F. Hussain, A. C. Stowe, C. Ramsey, and N. S. Dalal, Phys. Rev. Lett. **96**, 107202 (2006).
[10] A. C. Stowe, S. Nellutla, N. S. Dalal, and U. Kortz, Eur. J. Inorg. Chem. **19**, 3792 (2004).
[11] K. Y. Choi, N. S. Dalal, A. P. Reyes, P. L. Kuhns, Y. H. Matsuda, H. Nojiri, S. S. Mal, and U. Kortz, Phys. Rev. B **77**, 024406 (2008).
[12] S. Miyashita, and N. Nagaosa, Prog. Theor. Phys. **106**, 533 (2001).
[13] H. De Raedt, S. Miyashita, K. Michielsen, and M. Machida, Phys. Rev. B **70**, 064401 (2004).
[14] U. Kortz, N. K. Al-Kassem, M. G. Savelieff, N. A. Al Kadi, and M. Sadakane, Inorg. Chem. **40**, 4742 (2001).
[15] M. Bösing, I. Loose, H. Pohlmann, and B. Krebs, Chem. Eur. Jour **3**, 1232 (1997).
[16] M. J. Cooper and R. Nathans, Acta Cryst. **23**, 357 (1967).
[17] J. R. D. Copley and J. C. Cook, Chem. Phys. **292**, 477 (2003).
[18] K. Iida, H. Ishikawa, T. Yamase, and T. J. Sato, Jour. Phys. Soc. Jpn. **78**, 114709 (2009).
[19] P. J. Brown, *International Tables for Crystallography* (Springer, Netherlands, 2002) Vol. C, Chap. 4.4.
[20] From the INS spectrum of deuterated powder Cu_3 at $T = 1.5$ K measured at DCS with $E_i = 2.27$ meV (not shown), the parameters of the deuterated powder sample are determined by the excitations $\hbar\omega_1$ and $\hbar\omega_2$ as follows; $J^x_{1,2}/\mathrm{K} = -4.30 \pm 0.06$, $J^z_{1,2}/\mathrm{K} = -3.98 \pm 0.12$, $J^x_{2,3}/\mathrm{K} = -4.18 \pm 0.03$, $J^z_{2,3}/\mathrm{K} = -4.35 \pm 0.06$, $D^z_{1,2}/\mathrm{K} = 0.66 \pm 0.02$, and $D^x_{1,2}/\mathrm{K} = 0.37 \pm 0.14$. The values are almost the same as the values of the non-deuterated powder sample (see Eq. (2)). Thus, we can conclude that the deuterated Cu_3 spin cluster has almost same energy scheme as the non-deuterated Cu_3 spin cluster.